Affine Moment Invariants of Tensor Fields

Jan Flusser[1], Tomáš Suk[1(✉)], Matěj Lébl[1], Roxana Bujack[2],
and Ibrahim Ibrahim[3]

[1] Czech Academy of Sciences, Institute of Information Theory and Automation,
Pod Vodárenskou věží 4, 182 08 Praha 8, Czech Republic
{flusser,suk,lebl}@utia.cas.cz
[2] Data Science at Scale Team, Los Alamos National Laboratory, P.O. Box 1663,
Los Alamos, NM 87545, USA
bujack@informatik.uni-leipzig.de
[3] MR Unit, Department of Diagnostic and Interventional Radiology,
Institute for Clinical and Experimental Medicine IKEM, Vídeňská 1958/9,
140 21 Praha 4, Czech Republic
ibib@ikem.cz

Abstract. Tensor fields (TF) are a special kind of multidimensional
data, in which a tensor is given for each point in space. Often, it is a
3×3 array in each voxel. To detect the patterns of interest in the field,
special matching methods must be developed. We propose a method for
the description and matching of TF patterns under an unknown affine
transformation of the field. Transformations of TFs act not only in the
spatial coordinates but also on the field values, which makes the detec-
tion more challenging. To measure the similarity between the template
and the field patch, we propose original invariants with respect to affine
transformations designed from moments. Their performance is demon-
strated by experiments on real data from diffusion tensor imaging.

Keywords: Tensor field · affine invariants · template matching

1 Introduction

A gray-level image can be described by a scalar function. Sometimes, we need a
vector defined in each point of the space, then we talk about a vector field. An
example can be wind or water flow in a river. There are even more complicated
cases, where we need a tensor of rank 2 or higher in each point. An example is the
Cauchy stress tensor, where in each point of space, we need information not only

about magnitude of the inner force and its direction, but also about transverse components of the force that try to turn the inner part of the material.

Another example comes from diffusion tensor imaging (DTI). DTI is a modern technique based on magnetic resonance imaging (MRI) for an examination of tissues with internal anisotropic structure, such as neural axons of white matter in the brain and peripheral nerve fibres. It reconstructs the diffusion of water molecules in each voxel by measuring their movement in several distinct directions. This measurement is accomplished via several diffusion-weighted acquisitions, each obtained with a different orientation of the diffusion sensitizing gradients. After obtaining a complete set of such measurements (six diffusion-encoding gradient directions are the minimum needed to calculate the diffusion tensor; usually 30, 64, or more gradient directions are used), a symmetric second-rank 3×3 tensor is calculated in each voxel. This tensor image is an extremely useful modality, because it offers a possibility to detect a subtle pathology in the brain, to track neural tracts through the brain (this process is called tractography), to examine the integrity of peripheral nerves, and to diagnose of many neurological diseases [1,9,30].

In this paper, we deal with the template matching problem. A template, extracted from a reference image, shall be localized in the sensed image. However, there might be a deformation between the template and the corresponding patch. Template matching is an important part of registration of data taken at different times and in localization of regions of interest. Due to the tensorial nature of DTI data, common algorithms known from scalar image template matching cannot be used directly.

To measure the similarity between the template and the field patch, we need special kinds of descriptors, that are invariant to particular deformation of the template, to the template size and orientation. In this paper, we model the template variations by a *total affine transform*, which means that the transformation acts in the coordinate domain as well as in the value (vector or tensor) domain. This model is sufficiently general to capture most of the situations that appear in practice and, at the same time, it is still sufficiently simple to be handled mathematically.

2   Literature Survey

Our research is a follow-up of the previous work on the rotation and affine invariants of images and vector fields. The rotation invariants of vector fields were first studied by Schlemmer et al. [23]. Liu and Ribeiro [19] used them to detect singularities on meteorological satellite images showing wind velocity and Liu and Yap [18] applied them to the indexing and recognition of fingerprint images.

A generalization to more than two dimensions using tensor contraction was proposed by Langbein and Hagen [17]. Bujack et al. [5] showed that the invariants can be derived also by means of the field normalization approach. Yang et al. improved the numerical stability of the invariants by using orthogonal Gaussian-Hermite [33] and Zernike [32] moments. Recently, Bujack [3] introduced a *flexible*

basis of the invariants to avoid moments that vanish on the given templates. In [6], Bujack et al. propose the systematic approach to the generation of the tensor field invariants.

In contrast to the above group of papers on vector field rotation invariants, *affine moment invariants* (AMI) of graylevel images have been studied in hundreds of papers and books [13, 21, 22, 24, 25, 27]. Special AMIs were proposed for color images [7, 20, 26]. The most recent paper on this field is [16], where affine invariants of 2D vector fields are proposed.

In this paper, we focus on the case of 3D tensor fields. We restrict ourselves to the case of the second-rank symmetric tensors and we assume the inner (tensor values) and outer (coordinate) affine transformations are the same. Both assumptions are implied by physics of DTI. However, the presented theory of invariants could be developed in a more general way even without these limitations.

3   Affine Tensor Field Moment Invariants

Intuitively speaking, a tensor is an array of numbers, where the number of indices is called its *rank* and their range of the indices its *dimension*. If a tensor has a rank r and a dimension d, it has d^r components[1]. Unlike usual arrays, the tensors have two types of indices, contravariant and covariant. They differ in behavior under affine transformations of the space. The tensors are multiplied with the matrix of the direct transformation on behalf of each covariant index and by the matrix of the inverse transformation on behalf of each contravariant index. Formally, the tensor $\boldsymbol{\sigma}$ in affine transformation behaves

$$\sigma'^{i_1 i_2 \cdots i_n}_{j_1 j_2 \cdots j_m} = a^{\ell_1}_{j_1} a^{\ell_2}_{j_2} \cdots a^{\ell_m}_{j_m} \bar{a}^{i_1}_{k_1} \bar{a}^{i_2}_{k_2} \cdots \bar{a}^{i_n}_{k_n} \sigma^{k_1 k_2 \cdots k_n}_{\ell_1 \ell_2 \cdots \ell_m} ,$$

$$i_1, i_2, \ldots, i_n, j_1, j_2, \ldots, j_m, k_1, k_2, \ldots, k_n, \ell_1, \ell_2, \ldots, \ell_m = 1, 2, \ldots, d, \tag{1}$$

where a^k_j are elements of the matrix of the direct affine transformation $\mathbf{A}$ and $\bar{a}^i_\ell$ are elements of the matrix of the inverse affine transformation $\mathbf{A}^{-1}$. Here $i_1, i_2, \ldots, i_n$, $k_1, k_2, \ldots, k_n$ are contravariant indices, n is *contravariant rank*, $j_1, j_2, \ldots, j_m$, $\ell_1, \ell_2, \ldots, \ell_m$ are covariant indices, m is *covariant rank* and $r = n + m$ is *total rank* or just *rank*.

Special cases include scalars, which are tensors of rank zero, vectors, which are tensors of rank one, and matrices, which are tensors of rank two. The dimension and rank of tensor fields used in practice is limited. The most common tensor fields in physics are Cauchy stress tensor, viscous stress tensor, diffusion tensor and Maxwell stress tensor. All of them have dimension three and contravariant rank two, i.e. they form 3×3 arrays in each point of the 3D space

$$\boldsymbol{\sigma} \in \mathbb{R}^{3 \times 3}. \tag{2}$$

---

[1] This rank differs from the rank of matrix in linear algebra. Alternatively, it is called "order", but it can be confused with moment order. In this paper, we work with the moment order, but not with matrix rank, therefore we use rank here for the number of tensor indices.

The Cauchy stress tensor describes internal stress at a point inside a solid material. It is symmetric, i.e. $\boldsymbol{\sigma}^{ij} = \boldsymbol{\sigma}^{ji}$, so, it contains only six degrees of freedom. The diagonal components express magnitude and direction, while the other components of the tensor express the transverse components of the inner stress. A description of the tensors and operations with them can be found in [2] or in [8]. A good explanation can also be found in [10] or in its English translation [11].

Unlike matrices, tensors are multiplied in following fashion:

$$\boldsymbol{\sigma_p}^{ijk\ell} = \boldsymbol{\sigma_1}^{ij}\boldsymbol{\sigma_2}^{k\ell}, \ i, j, k, \ell = 1, \ldots, 3, \tag{3}$$

where $\boldsymbol{\sigma_p} \in \mathbb{R}^{3\times3\times3\times3}$ i.e. each component of the first tensor is multiplied with each component of the second tensor. The tensor product is noted as

$$\boldsymbol{\sigma_p} = \boldsymbol{\sigma_1} \otimes \boldsymbol{\sigma_2}. \tag{4}$$

The product has four indices, thus it is not a second rank tensor, but it satisfies the general definition of a tensor.

Two Cauchy stress tensors can be added

$$\boldsymbol{\sigma_s}^{ij} = \boldsymbol{\sigma_1}^{ij} + \boldsymbol{\sigma_2}^{ij} \ i, j = 1, \ldots, 3, \tag{5}$$

i.e. only corresponding components are added. The result $\boldsymbol{\sigma_s} = \boldsymbol{\sigma_1} + \boldsymbol{\sigma_2}$ is again a second rank tensor. Please note that this product and sum extend to tensors of all ranks. For a formal introduction to general tensors, we recommend [4].

The viscous stress tensor is analogous to the Cauchy stress tensor in fluids. Unlike the Cauchy stress tensor, it can have an antisymmetric component and is generally not symmetric. The Maxwell stress tensor is the analogon of the Cauchy stress tensor for electromagnetic forces. It is also symmetric.

An example from biology comes from diffusion tensor imaging. It is a way of using magnetic resonance imaging (MRI), which measures the restricted diffusion of water molecules in the tissue. The diffusion tensor $\mathbf{D} \in \mathbb{R}^{3\times3}$ is a second rank three-dimensional symmetric tensor, like the Cauchy stress tensor.

3.1   Covariant and Contravariant Indices

Generally, tensors have two types of indices - covariant and contravariant. The covariant indices are notated as subscripts, e.g. $\boldsymbol{\nu}_{ij}$, the contravariant indices are notated as superscripts, e.g. $\boldsymbol{\nu}^{ij}$.

The range of the indices equals the dimension d of the space, i.e. $i = 1, 2$ in 2D and $i = 1, 2, 3$ in 3D. Let $A \in \mathbb{R}^{d\times d}$ be a matrix representing an affine transformation. A tensor of covariant rank two behaves under the transformation A as

$$\boldsymbol{\nu'}_{ij} = \sum_{k=1}^{d}\sum_{\ell=1}^{d}\mathbf{A}_i^k\mathbf{A}_j^\ell\boldsymbol{\nu}_{k\ell}. \tag{6}$$

Similarly for a tensor of contravariant rank two, we have

$$\boldsymbol{\nu'}^{ij} = \sum_{k=1}^{d}\sum_{\ell=1}^{d}(\mathbf{A}^{-1})_k^i(\mathbf{A}^{-1})_\ell^j\boldsymbol{\nu}^{k\ell}. \tag{7}$$

The most popular second rank tensor, probably known from linear algebra, is a matrix denoting a linear transform. It has both covariant and contravariant indices and transforms via

$$\boldsymbol{\nu'}_i^j = \sum_{k=1}^{d}\sum_{\ell=1}^{d}\mathbf{A}_i^k(\mathbf{A}^{-1})_\ell^j\boldsymbol{\nu}_k^\ell, \tag{8}$$

which is equivalent to the common matrix transformation $\mathbf{A}\boldsymbol{\nu}\mathbf{A}^{-1}$.

3.2   Contraction

There is another important operation with tensors - the contraction. It is the sum over two indices, one covariant and one contravariant. Let us take such a tensor $\boldsymbol{\nu}_i^j$. Its contraction equals

$$c = \sum_{i=1}^{d}\boldsymbol{\nu}_i^i, \tag{9}$$

which is equivalent to the trace of the matrix. In so-called Einstein notation [31], the symbol of sum is omitted and we write just $c = \boldsymbol{\nu}_i^i$. The contraction is sometimes noted

$$c = \sum_{(i,j)}\boldsymbol{\nu}_i^j. \tag{10}$$

It means the sum is performed over the summands satisfying $i = j$.

They key property used in this paper is the invariance of the total contraction to affine transformations. If we observe the contraction of a tensor $\boldsymbol{\nu}_i^j$ subject to an affine transformation, we obtain

$$\sum_{i=1}^{d}\boldsymbol{\nu'}_i^i = \sum_{i=1}^{d}\sum_{k=1}^{d}\sum_{\ell=1}^{d}\mathbf{A}_i^k(\mathbf{A}^{-1})_\ell^i\boldsymbol{\nu}_k^\ell = \sum_{i=1}^{d}\boldsymbol{\nu}_i^i = c. \tag{11}$$

Thanks to the common index i, the matrices $\mathbf{A}$ and $\mathbf{A}^{-1}$ are multiplied as matrices, the result is an identity matrix and the contraction remains unchanged regardless the transformation. The contraction is the way to affine invariants. When we can compute a total contraction (i.e. contractions over all indices) of a tensor, it is an affine invariant.

3.3   Transformations of Tensor Fields

Now, let us look at an actual tensor field

$$\boldsymbol{\sigma}(x,y,z) \in \mathbb{R}^{3\times3} \tag{12}$$

assigning a tensor to each point in space. Sometimes, it is noted as

$$\boldsymbol{\sigma}(\mathbf{x}), \tag{13}$$

where $\mathbf{x} = (x,y,z)^T = (x^1,x^2,x^3)^T$ is the vector of coordinates.

As mentioned above, for transforming tensor fields (as for vector field) we need to define two transformations. One for transforming the coordinate system, the second one transforms the tensor (vector) values. Usually these transformations are identical resulting in intuitive transformation, e.g. rotating the tensor (vector) field also rotates the directions of tensors (vectors). Formally let $\mathbf{A}$, $\mathbf{B}$ be these two affine transformations acting on a tensor field

$$\boldsymbol{\sigma}'(\mathbf{x}') = \mathbf{B}(\boldsymbol{\sigma}(\mathbf{A}^{-1}(\mathbf{x}))). \tag{14}$$

We can write the transformations using their 3×3 matrix representations, which we also denote by $\mathbf{A}$, $\mathbf{B}$. Here, the inner transformation of the coordinates takes the form

$$\mathbf{x}'^i = \sum_{(j,k)} (\mathbf{A}^{-1} \otimes \mathbf{x})_k^{ij} = (\mathbf{A}^{-1})_j^i \mathbf{x}^j, \tag{15}$$

which coincides with the standard matrix vector product in matrix notation $\mathbf{A}^{-1}\mathbf{x}$. The outer transformation of the tensor values is written as

$$\boldsymbol{\sigma}'^{kl} = \sum_{\substack{(i,m) \\ (j,n)}} (\mathbf{B} \otimes \mathbf{B} \otimes \boldsymbol{\sigma})_{ij}^{k\ell mn} = \{\mathbf{B}_i^k \mathbf{B}_j^\ell \boldsymbol{\sigma}^{ij}\} \tag{16}$$

using contraction and Einstein notation.

The case $\mathbf{A} = \mathbf{B}$ is called the total transformation, cases where transformations differ are rare. The same way the tensor multiplication together with contraction in the inner transformation (15) equals the matrix multiplication, the outer transformation (16) can be rewritten to the matrix multiplication as

$$\boldsymbol{\sigma}' = \mathbf{B}\boldsymbol{\sigma}\mathbf{B}^T. \tag{17}$$

Note that affine transformation does not change the rank of a tensor.

3.4   Moment Tensors

Geometric moments of a real valued function $f(x,y)$ have been introduced to pattern recognition in [14]

$$m_{pq} = \int\limits_{-\infty}^{\infty} \int\limits_{-\infty}^{\infty} x^p y^q f(x,y)\, \mathrm{d}x\, \mathrm{d}y. \tag{18}$$

The sum $o = p+q$ is called *order* of the moment. For a 3D tensor field, we simply extend (18) by the third spatial coordinate and replace the scalar function f by our tensor valued function σ^{ij}

$$m_{pqr}^{(ij)} = \int\limits_{-\infty}^{\infty} \int\limits_{-\infty}^{\infty} \int\limits_{-\infty}^{\infty} x^p y^q z^r \sigma^{ij}(x,y,z)\, \mathrm{d}x\, \mathrm{d}y\, \mathrm{d}z. \tag{19}$$

The moments of order o can be arranged to the *moment tensor* ${}^o\mathbf{M}$. For general tensors we have

$$
{}^o\mathbf{M}^{k_1\ldots k_o i_1\ldots i_n}_{j_1\ldots j_m} = \int_{\mathbb{R}^d} x^{k_1}\cdots x^{k_o}\sigma^{i_1\ldots i_n}_{j_1\ldots j_m}(x^1\cdots x^d)\,\mathrm{d}^d x, \tag{20}
$$

where o is the order of the moment tensor, m is the covariant rank of the tensor field and n is its contravariant rank[2]. For example, the moment tensor of a Cauchy stress tensor is

$$
{}^o\mathbf{M}^{k_1\ldots k_o ij} = \int_{-\infty}^{\infty}\int_{-\infty}^{\infty}\int_{-\infty}^{\infty} x^{k_1}\cdots x^{k_o}\boldsymbol{\sigma}^{ij}(x^1,x^2,x^3)\,\mathrm{d}x^1\mathrm{d}x^2\mathrm{d}x^3. \tag{21}
$$

Also note that the components of the moment tensor equal the geometric moments

$$
{}^o\mathbf{M}^{k_1\ldots k_o i_1\ldots i_n}_{j_1\ldots j_m} = m^{(i_1\ldots i_n)}_{p_1\ldots p_d(j_1\ldots j_m)} \tag{22}
$$

iff p_ℓ many of the indices $k_1,\ldots,k_o$ equals ℓ for all $\ell = 1,\ldots,d$.

3.5   Construction of the Invariants

The affine invariants can be constructed as total contractions of tensor products of moment tensors and permutation tensors [11]. The *permutation tensor* ε in 2D takes the form

$$
\varepsilon_{ij} = \begin{pmatrix} 0 & 1 \\ -1 & 0 \end{pmatrix}. \tag{23}
$$

In 3D, it is the $3\times 3\times 3$ cube with slices

$$
\varepsilon_{ij1} = \begin{pmatrix} 0 & 0 & 0 \\ 0 & 0 & 1 \\ 0 & -1 & 0 \end{pmatrix}, \ \varepsilon_{ij2} = \begin{pmatrix} 0 & 0 & -1 \\ 0 & 0 & 0 \\ 1 & 0 & 0 \end{pmatrix}, \ \varepsilon_{ij3} = \begin{pmatrix} 0 & 1 & 0 \\ -1 & 0 & 0 \\ 0 & 0 & 0 \end{pmatrix}. \tag{24}
$$

If the index values create a cyclic shift of 123, the value is 1, if it is a cyclic shift of 321, the value is -1. In the remaining 21 positions, the value is 0.

An example of such an invariant is

$$
I = \sum_{\substack{(i_1,i_2)(j_1,j_2)(j_1,j_2) \\ (k_1,k_2)(\ell_1,\ell_2)(m_1,m_2) \\ (n_1,n_2)(o_1,o_2)(p_1,p_2)}} {}^2\mathbf{M}^{i_1 j_1 k_1 \ell_1} \otimes {}^1\mathbf{M}^{m_1 n_1 o_1} \otimes {}^0\mathbf{M}^{p_1 q_1} \otimes \varepsilon_{i_2 k_2 n_2} \otimes \varepsilon_{j_2 m_2 p_2} \otimes \varepsilon_{\ell_2 o_2 q_2} =
$$

$$
= {}^2\mathbf{M}^{ijk\ell}\, {}^1\mathbf{M}^{mno}\, {}^0\mathbf{M}^{pq}\varepsilon_{ikn}\varepsilon_{jmp}\varepsilon_{\ell oq}. \tag{25}
$$

If we need to generate all the affine invariants of a tensor field, we need to generate all total contractions of the type of Eq. (25), i.e. all tensor products of all moment tensors and permutation tensors, where each index is used exactly twice, once in the moment tensor and once in the permutation tensor.

---

[2] Here x^{k_1} is not power, but upper index (superscript), i.e. if $k_1 = 3$, then $x^{k_1} = z$. We multiply o coordinates in the integral.

3.6   Tensor Field Affine Moment Invariants and Quadri-Layer Hypergraphs

Not all combinations are needed to unambiguously describe a template. We are looking for a subset that is *complete*, i.e., it has enough invairiants to discern two templates that differ something other than an affine transform, but has as little elements as possible to maximize efficiency. When we want to generate a complete set of affine invariants, we must generate all possible combinations of moment tensors and permutation tensors and also all possible total contractions on the given combinations.

We can help us with the idea of graphs, where each node corresponds to a moment tensor and each edge to a permutation tensor. When we generate all the graphs with the given parameters and compute the corresponding invariants, we obtain the complete set. In the case of tensor field affine moment invariants (TFAMIs), we need so-called *quadri-layer hypergraphs*. Let $G = (\mathcal{V}; E))$ be a graph consisting of a set of vertices (nodes) $\mathcal{V}$ and a set of edges E.

In standard graphs, each edge connects two nodes. In the hypergraph, each edge can connect multiple nodes. Similarly, in the standard graph, all edges are qualitatively equal but sometimes we need more types of edges. Such graphs are called multilayer graphs.

In the case of symmetric 3D tensor fields, we need quadri-layer hypergraphs, where each edge connects three nodes. We note it

$$G = (\mathcal{V}; E_1, E_2, E_3, E_4).$$

Further we denote

$$G_k = (\mathcal{V}; E_k)$$

the *k-th layer* of the graph G.

An arbitrary invariant can be represented by a quadri-layer graph as follows. Each moment tensor in the product (25) corresponds to a graph node. Each permutation tensor ε_{ijk} corresponds to an edge connecting three nodes. It connects the moment tensor with the index i, the moment tensor with the index j, and the moment tensor with the index k.

The edges from E_1 use only coordinate indices, the edges from E_2 connect two coordinate indices and one value index, the edges from E_3 use one coordinate index and two value indices, and the edges from E_4 connect only value indices. The plotting of the triple edges of four types is not easy; we decided to denote them as tripods with color arms. The black arm means the coordinate index, while the contravariant value index is noted by magenta color. The examples of the color combinations are in Fig. 1.
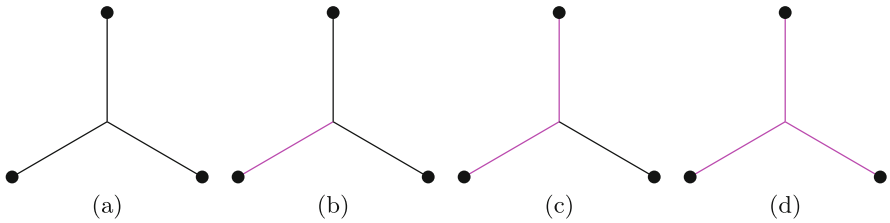
Fig. 1. Examples of triple hyperedges of individual types: (a) E_1 connecting only coordinate indices, (b) E_2 connecting two coordinate indices and one value index (c) E_3 connecting one coordinate index and two value indices, and (d) E_4 connecting only value indices.

We can use different types of graphs, but this type proved its efficiency in the invariant generation. In Fig. 2, we can see the graph representing the invariant (25). We can observe a node with two black edges, a node with one black edge and a node without black edges. They correspond to the moments of orders 2, 1, and 0 respectively. All the nodes has two magenta edges corresponding to the value indices, because we work with the tensors of the second rank.

An algorithm for a systematic generation of all such graphs can be found on the webpage [28]. In Table 1, there are the numbers of the generated invariants. Here, # edges is the number of edges permitted, # graphs denotes the overall possible number of configurations that produce affine invariants, # invariants represents the number to which we could reduce the set while maintaining its completeness, and # independent is the theoretically possible lower limit of independent affine invariants.

Table 1. The numbers of graph edges, graphs, all invariants, and independent invariants.

# edges	# graphs	# invariants	# independent
3	635	1	1
4	14941	12	12
5	404448	41	40
6	11862154	2123	152
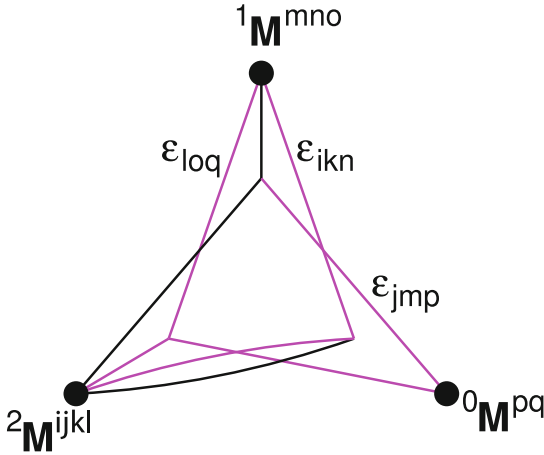
Fig. 2. The graph representing invariant from Eq. (25).

4   Numerical Experiment

We tested our method on real world data obtained from a diffusion MRI scan of a human head. The diffusion in the brain is represented by a three-dimensional second rank symmetric tensor field. Example slices of those data are shown in Fig. 3, where the 3×3 tensor in each pixel is visualized through color coding as described in the following section.

4.1   Obtaining Data and Visualization

In this experiment, we used real DTI scans of a human brain. The device used for an examination was a 3T Siemens TrioTim MR scanner using spin-echo echo-planar imaging (SE EPI) sequence. The acquisition parameters were the following: repetition time (TR) of 8300 ms, echo time (TE) of 84 ms, voxel size of $2 \times 2 \times 2$ mm, 68 axial slices, two averages, field of view (FOV) of 256 mm, number of diffusion directions 30, two b-values: 0, and $900 \, \text{s/mm}^2$. The output of the machine are 62 measurements each with different gradient settings. One measurement is a set of 68 slices in the axial plane with a of resolution 112×128 pixels resulting in 62 $112 \times 128 \times 68$ volumes, each representing the diffusion in a certain direction. These volumes can be stacked together (as described in [15]) to produce a 3D volume with of 3×3 symmetric matrices - one tensor in each voxel.

It is challenging to visualize such data [12]. We used a method, where we visualize the tensor field so that colors are used to indicate the direction of the diffusion. First, we assign the RGB colors to the world coordinates x, y, z i.e. red for the coronal, green for the sagittal and blue for the axial plane. Then for each voxel, the diffusion tensor is transformed into a diagonal matrix. Components on the diagonal - eigenvalues - represent a magnitudes of diffusion in

a new coordinate system given by the corresponding eigenvectors. This efficiently transfers a tensor into a vector. Each of the new coordinates can be assigned a color based on the $x, y, z \iff R, G, B$ correspondence. Finally, the three colors can be merged into one as their linear combination with coefficients being the corresponding eigenvalues.

For clarity, only the voxels with strongly anisotropic diffusion (one prevailing direction of diffusion) were colored, while the rest was assigned gray level based on the fractional anisotropy (scalar value, the total diffusion).

(a)   (b)   (c)
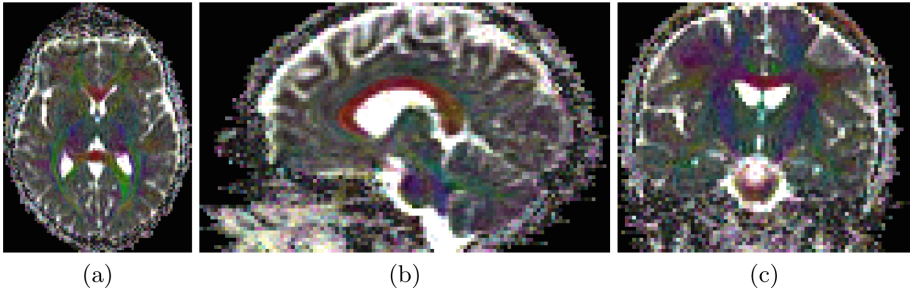
Fig. 3. Original MRI diffusion tensor, cut in (a) axial, (b) sagittal and (c) coronal plane. (Color figure online)

4.2   Invariance

We generated ten random affine transformations without translation. They were composed of two rotations (Euler angles with uniform distribution on the intervals $\langle 0, 2\pi \rangle$, $\langle 0, \pi \rangle$, and $\langle 0, 2\pi \rangle$) and a non-uniform scaling (Gauss distribution with mean one and standard deviation 0.2) between them. An example of such an affine transformation is shown in Fig. 4. The values of four representative invariants are depicted in Fig. 5. The horizontal lines show that they indeed do not change under the different affine transforms. The labels on the horizontal axis note specific affine transformations, 0 are values of the original tensor field. The average relative error over all invariants and all affine transformations is 1.043%. For comparison, we also converted the moments directly, without re-sampling the tensor field. The relative average error then decreased to $1.2604 \cdot 10^{-12}$ %. It is caused just by numerical imprecisions during computation.

4.3   Template Matching

We tested our invariants in a template matching experiment. We generated 10 random spherical templates with a diameter of 15 voxels (see Fig. 7 for an example of the template). At least 90% of the volume of all the templates is inside the patient's head (i.e. valid data) and there is no overlap between them. Then, we again generated two random affine transformations of the whole diffusion tensor field and searched the templates in them.

(a)   (b)   (c)
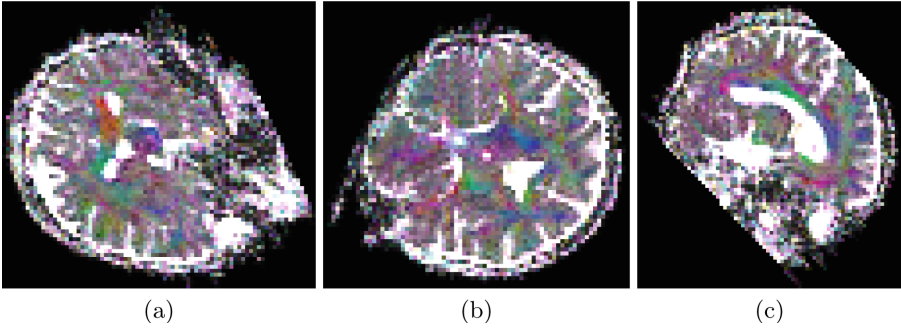
Fig. 4. The MRI diffusion tensor field from Fig. 3 after an example affine transformation, cut in (a) x-y plain, x-z plain, (c) y-z plain. The color coding is descibed in the main text. The artifacts are part of the data and have nothing to do with the transformation. (Color figure online)
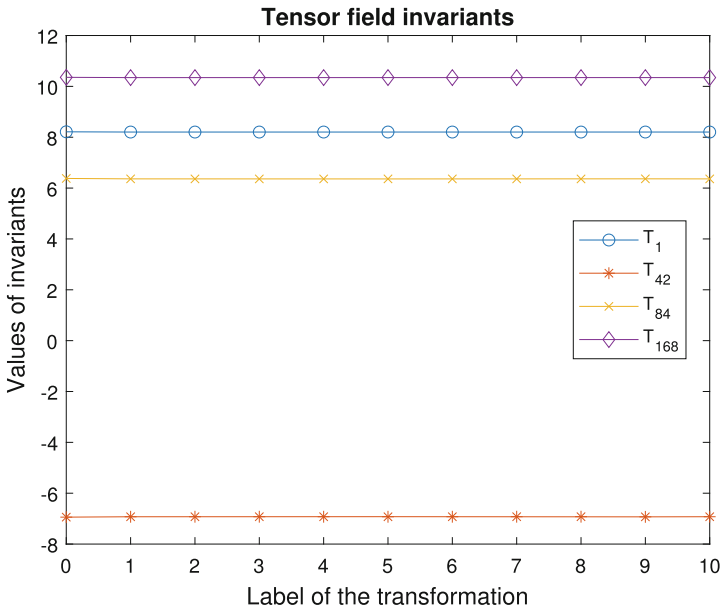
Fig. 5. Values of some TFAMI.

We searched the tensor field voxel by voxel, computed TFAMIs in each position, and tested for a match with TFAMIs of the templates. We used 205 invariants of symmetric tensor fields from the 2nd to the 6th order, their list can be downloaded from [29]. The sorted errors can be seen in Fig. 6. The errors are computed as Euclidean distances of the affinely transformed template positions and the best matches of TFAMIs.
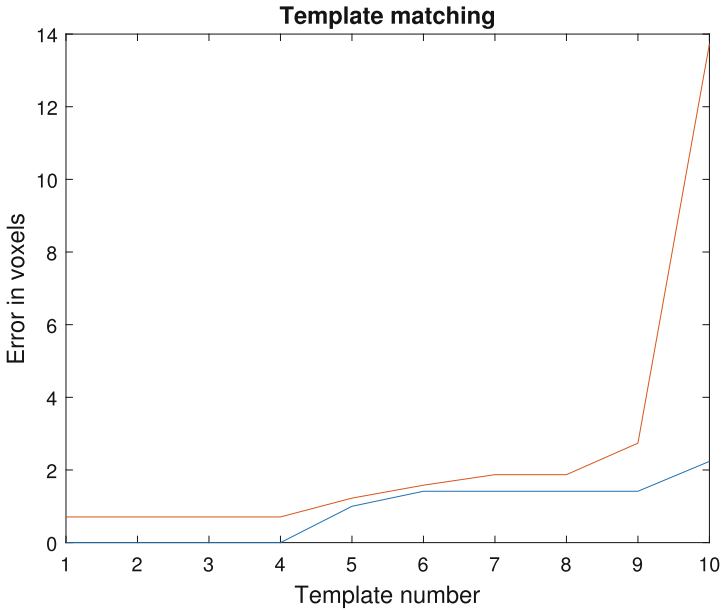
Fig. 6. Errors in the two template matching experiments. Each line corresponds to a random affine transform.

We consider errors greater than 5 voxels as failures. So, the templates in the first transformation were found successfully, while in the second attempt, we encountered one mismatch. This template size is a limit, where the mismatches are rare. The templates of a bigger size are found reliably, while the matching of smaller templates fails frequently because of a shortage of significant information contained in the template. We intentionally chose limit parameter values, where we can study the behavior of the invariants. When we use bigger templates, we obtain errorless result.

(a)   (b)   (c)
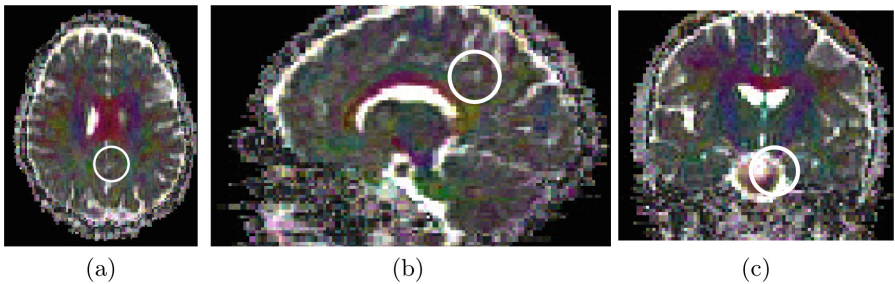
Fig. 7. MRI diffusion tensor with example of a template, (a) x-y plain, x-z plain, (c) y-z plain. The color coding is described in the main text. (Color figure online)

5   Conclusion

This paper introduced invariants of tensor fields w.r.t. total affine transformations based on the moments of tensor fields. The behavior of tensor fields in affine transformations is different from vector fields, scalar fields, and color images and the traditional techniques cannot be used. We developed a set of complete invariants that allow affine invariant pattern detection on second order tensor fields and demonstrated their performance on MRI diffusion tensor fields.

References

1. Alexander, A.L., Lee, J.E., Lazar, M., Field, A.S.: Diffusion tensor imaging of the brain. Neurotherapeutics **4**(1), 316–329 (2007)
2. Bowen, R., Wang, C.: Introduction to Vectors and Tensors. Dover books on mathematics, Dover Publications, Mineola, New York (2008)
3. Bujack, R., Flusser, J.: Flexible basis of rotation moment invariants. In: WSCG, pp. 11–20 (2017)
4. Bujack, R., Hagen, H.: Moment invariants for multi-dimensional data. In: Schultz, T., Özarslan, E., Hotz, I. (eds.) Modeling, Analysis, and Visualization of Anisotropy. MV, pp. 43–64. Springer, Cham (2017). https://doi.org/10.1007/978-3-319-61358-1_3
5. Bujack, R., Hlawitschka, M., Scheuermann, G., Hitzer, E.: Customized TRS invariants for 2D vector fields via moment normalization. Pattern Recogn. Lett. **46**(1), 46–59 (2014)
6. Bujack, R., Zhang, X., Suk, T., Rogers, D.: Systematic generation of moment invariant bases for 2D and 3D tensor fields. Pattern Recogn. **123**, 108313 (2022)
7. Gong, M., Hao, Y., Mo, H., Li, H.: Naturally combined shape-color moment invariants under affine transformations. Comput. Vis. Image Underst. **162**, 46–56 (2017)
8. Grinfeld, P.: Introduction to Tensor Analysis and the Calculus of Moving Surfaces. Springer, New York (2013)
9. de Groot, M., et al.: White matter degeneration with aging: longitudinal diffusion MR imaging analysis. Radiology **279**(2), 532–541 (2015)
10. Gurevich, G.B.: Osnovy teorii algebraicheskikh invariantov. Moskva, The Union of Soviet Socialist Republics, OGIZ (1937)
11. Gurevich, G.B.: Foundations of the theory of algebraic invariants. Nordhoff, Groningen, The Netherlands (1964)
12. Hergl, C., et al.: Visualization of tensor fields in mechanics. Comput. Graph. Forum **40**(6), 135–161 (2021)
13. Hickman, M.S.: Geometric moments and their invariants. J. Math. Imaging Vis. **44**(3), 223–235 (2012)
14. Hu, M.K.: Visual pattern recognition by moment invariants. IRE Trans. Inf. Theory **8**(2), 179–187 (1962)
15. Kingsley, P.B.: Introduction to diffusion tensor imaging mathematics: Part i–iii. Concepts Magn. Reson. Part A **28**(2), 101–179 (2006)
16. Kostková, J., Suk, T., Flusser, J.: Affine invariants of vector fields. IEEE Trans. Pattern Anal. Mach. Intell. **43**(4), 1140–1155 (2021)
17. Langbein, M., Hagen, H.: A generalization of moment invariants on 2D vector fields to tensor fields of arbitrary order and dimension. In: Bebis, G., et al. (eds.) ISVC 2009. LNCS, vol. 5876, pp. 1151–1160. Springer, Heidelberg (2009). https://doi.org/10.1007/978-3-642-10520-3_110

18. Liu, M., Yap, P.T.: Invariant representation of orientation fields for fingerprint indexing. Pattern Recogn. **45**(7), 2532–2542 (2012)
19. Liu, W., Ribeiro, E.: Detecting singular patterns in 2-D vector fields using weighted Laurent polynomial. Pattern Recogn. **45**(11), 3912–3925 (2012)
20. Mindru, F., Tuytelaars, T., Gool, L.V., Moons, T.: Moment invariants for recognition under changing viewpoint and illumination. Comput. Vis. Image Underst. **94**(1–3), 3–27 (2004)
21. Reiss, T.H.: Recognizing Planar Objects Using Invariant Image Features. LNCS, vol. 676. Springer, Berlin, Germany (1993). https://doi.org/10.1007/BFb0017553
22. Rothe, I., Süsse, H., Voss, K.: The method of normalization to determine invariants. IEEE Trans. Pattern Anal. Mach. Intell. **18**(4), 366–376 (1996)
23. Schlemmer, M., et al.: Moment invariants for the analysis of 2D flow fields. IEEE Trans. Vis. Comput. Graph. **13**(6), 1743–1750 (2007)
24. Suk, T., Flusser, J.: Graph method for generating affine moment invariants. In: Proceedings of the 17th International Conference on Pattern Recognition ICPR'04, pp. 192–195. IEEE Computer Society (2004)
25. Suk, T., Flusser, J.: Affine moment invariants generated by automated solution of the equations. In: Proceedings of the 19th International Conference on Pattern Recognition ICPR'08. IEEE Computer Society (2008)
26. Suk, T., Flusser, J.: Affine moment invariants of color images. In: Jiang, X., Petkov, N. (eds.) CAIP 2009. LNCS, vol. 5702, pp. 334–341. Springer, Heidelberg (2009). https://doi.org/10.1007/978-3-642-03767-2_41
27. Suk, T., Flusser, J.: Affine moment invariants generated by graph method. Pattern Recogn. **44**(9), 2047–2056 (2011)
28. Suk, T., Flusser, J.: Afintensors - generation of invariants of tensor fields (2019). http://zoi.utia.cas.cz/afintensors
29. Suk, T., Flusser, J.: Affine moment invariants of tensor fields (2020). http://zoi.utia.cas.cz/affine-tensor-fields
30. Wheeler-Kingshott, C.A.M.G., et al.: Investigating cervical spinal cord structure using axial diffusion tensor imaging. Neuroimage **16**(1), 93–102 (2002)
31. Wikipedia: einstein notation (last edit 2022). http://en.wikipedia.org/wiki/Einstein_notation
32. Yang, B., Kostková, J., Flusser, J., Suk, T., Bujack, R.: Rotation invariants of vector fields from orthogonal moments. Pattern Recogn. **74**, 110–121 (2018)
33. Yang, B., Kostková, J., Suk, T., Flusser, J., Bujack, R.: Recognition of patterns in vector fields by Gaussian-Hermite invariants. In: Luo, J., Zeng, W., Zhang, Y.J. (eds.) International Conference on Image Processing ICIP'17, pp. 2350–2363. IEEE (2017)